NJC

ROYAL SOCIETY OF CHEMISTRY

PAPER

View Article Online
View Journal | View Issue

Cite this: *New J. Chem.*, 2020, **44**, 9377

The first-principles study of the adsorption of NH_3, NO, and NO_2 gas molecules on InSe-like phosphorus carbide†

Andrey A. Kistanov

Received 1st April 2020,
Accepted 12th May 2020

DOI: 10.1039/d0nj01612h

rsc.li/njc

The adsorption of environmental gas molecules, *i.e.*, NH_3, NO, and NO_2 on the γ-PC surface has been studied using first-principles calculations. The lowest-energy configurations of these molecules on the γ-PC surface were found and the adsorption energies were calculated. The NH_3, NO, and NO_2 molecules were found to be physisorbed on the γ-PC surface. The analysis of the charge transfer between the molecules and the surface predicted NH_3 and NO as donors to γ-PC, while NO_2 acted as an acceptor to γ-PC. Remarkable changes in the band structure of γ-PC were found upon the adsorption of NO_2 on its surface. In addition, significant modulations in the work function of γ-PC were observed after the adsorption of NH_3 and NO.

Introduction

Ultrathin two-dimensional (2D) materials possess a high surface area-to-volume ratio and weak screening of electrons, which make them vulnerable to the influence of the ambient physical and chemical adsorbates.[1,2] On the other hand, the advanced chemical activity of 2D materials offers the possibility to modify their electronic and chemical properties by the effect of ambient adsorbates.[3] The high sensitivity of the 2D materials to environmental molecules and gases also makes them promising for gas adsorption and detection.[4] For instance, first-principles calculations have predicted a strong binding of the NO and NO_2 gas molecules to MoS_2.[5] The MoS_2 monolayer produced by annealing sputtered Mo films in S vapor has shown excellent selectivity to NH_3.[6] Many investigations indicate potential for InSe in fabricating gas sensors.[7,8] Particularly, the strong ability of InSe to interact with external NH_3, NO_2, and NO molecules has been found.[9] It should be noted that the InSe surface degrades as a result of defect-photo-promoted oxidations, which may reduce its applications.[10]

The discovery of new 2D materials, such as phosphorene, has shown that these materials may provide much stronger adsorption ability to ambient molecules and gases compared to MoS_2 or InSe.[9,11–13] The promoted activity of phosphorene has been reported for the NO, NO_2, NH_3, and CO molecules.[14,15] In addition, the gas sensing ability of phosphorene has been improved by the doping of its surface by NH_3 and NO_2 gas molecules.[16] However, such high chemical activity of phosphorene leads to its fast degradation in ambient conditions.[17] In addition, the formation of defects on the phosphorene surface may lead to the degradation of its structure.[18] Nevertheless, the adsorption of different adatoms on phosphorene including s and p valence metals, 3d transition metals, noble metals, H and O does not necessarily disturb its structural integrity.[19,20]

In the search of 2D materials that are highly sensitive to gases while remaining structurally stable in ambient conditions, considerable research has focused on the study of 2D hybrid materials.[21] Phosphorus carbide (PC), a composite of graphene and phosphorene, is one of these materials.[22,23] The latest studies show that PC has an anisotropic structure, wide band gap, and high charge carrier mobility.[24] Furthermore, PC-based field-effect transistors have been fabricated recently *via* a novel carbon doping technique.[25] More importantly, PC combines the high chemical activity existing in phosphorene and the structural stability inherent to graphene, which are the most important features of all gas sensors.[24,26,27] Previous studies on the sensing mechanism of 2D layered materials, including monolayer MoS_2,[28–30] monolayer SnS_2,[31] and monolayer C_3N,[32] indicate that charge transfer plays an important role for the sensing of gas molecules.

Very recently, stable γ-PC with an InSe-like structure has been predicted theoretically.[33] This PC allotrope possesses the promoted adsorption and low diffusion barrier of Li, which render its application in rechargeable nanodevices. However, to date, the possible effects of ambient adsorbates on the structure and electronic properties of γ-PC as well as the suitability of γ-PC for gas detection have not been investigated.

In this work, first-principles calculations have been performed for the adsorption of NH_3, NO, and NO_2 molecules on γ-PC. Their exact configurations on the surface and their preferential binding

Nano and Molecular Systems Research Unit, University of Oulu, 90014 Oulu, Finland. E-mail: andrey.kistanov@oulu.fi

† Electronic supplementary information (ESI) available. See DOI: 10.1039/d0nj01612h

sites were determined by calculating their adsorption energy. In order to determine their effect on the electronic properties of γ-PC, the charge transfer and band structure analyses of molecule-adsorbed γ-PC were conducted.

Results and discussion

The top and side views of the unit cell of the optimized γ-InSe-like phosphorus carbide (γ-PC) are shown in Fig. 1a. The calculated lattice constants of γ-PC were a = 3.09 Å and b = 5.35 Å, and the lengths of the C–C and C–P bonds were 1.56 and 1.97 Å, respectively, which were comparable with those reported in the theoretical study of γ-PC.[33] The band structure of γ-PC obtained by the GGA PBE (black) and HSE06 (red) methods is presented in Fig. 1b. Importantly, both methods predicted γ-PC to be an indirect band gap semiconductor. The GGA PBE approach only slightly underestimated the band gap value (1.51 eV) compared to that (2.58 eV) calculated using the HSE method, which was also consistent with previously reported results.[33] Therefore, the less expensive computational method was used in this work.

To determine the lowest-energy adsorption position of the NH_3, NO, and NO_2 molecules on γ-PC, several possible configurations of the molecules in all possible adsorption sites and aligned parallel, perpendicular or tilted to the surface plane of γ-PC were investigated. The calculated adsorption energy (E_a) values of NH_3, NO, and NO_2 on γ-PC, the charge transfer (Δq) between the adsorbed molecules and the γ-PC surface, the shortest distance (d) from the adsorbed molecules to the γ-PC surface, and the work function of the molecule-adsorbed γ-PC for the most stable adsorption configurations are given in Table 1. Several other examined configurations of the considered molecules on γ-PC with comparably lower E_a are shown in Fig. S1–S3 (see ESI†) and the E_a, d, and Δq values for these structures are presented in Table S1 (see ESI†).

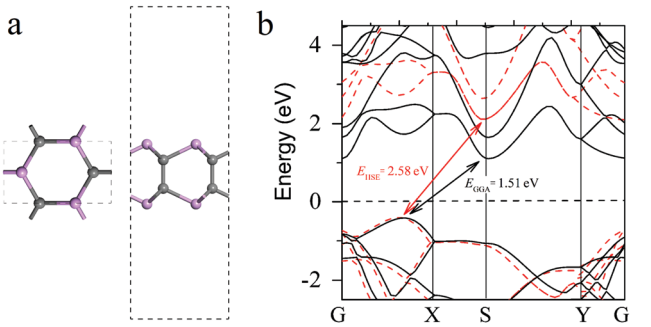

Fig. 1 (a) The top and side views of the unit cell and (b) GGA PBE (the black line) and HSE (the red line) band structures of γ-PC.

Table 1 The adsorption energy (E_a) of NH_3, NO, and NO_2 on γ-PC and $MoS_2$34 and InSe[9] (reference data); the charge transfer (Δq) between the adsorbed molecules and the γ-PC surface; the shortest distance (d) from the adsorbed molecules to the γ-PC surface; the work function (WF) of molecule-adsorbed γ-PC

Molecule	E_a, eV MoS_2	E_a, eV InSe	E_a, eV γ-PC	Role	Δq, e	d, Å	WF, eV
NH_3	−0.49	−0.20	−0.17	Donor	−0.028	2.90	5.46
NO	−0.54	−0.13	−0.20	Donor	−0.003	3.01	4.71
NO_2	−0.94	−0.24	−0.55	Acceptor	0.091	2.88	5.61
No molecule	—	—	—	—	—	—	5.61

NH_3 adsorption

The lowest-energy configuration of an NH_3 molecule on the γ-PC surface is shown in Fig. 2a. The molecule was located above the centre of the hollow hexagon with the three H atoms pointing away from the surface. After adsorption, the shortest distance (d) between the N atom of the molecule and the surface was 2.90 Å, and the H–N bonds elongated to 1.023 Å compared to those of a free NH_3 gas molecule (1.01 Å). This elongation of bond lengths was mostly attributed to the transfer of electron density from the old bonds to the newly formed bonds between NH_3 and γ-PC.[35] The adsorption energy (E_a) of the NH_3 molecule on the γ-PC surface was −0.17 eV, which suggested that the physisorption behaviour of NH_3 on γ-PC was similar to that of NH_3 on InSe (E_a = −0.20 eV);[9] however, on MoS_2, the NH_3 molecule possessed about 2 times lower E_a (−0.49 eV).[34]

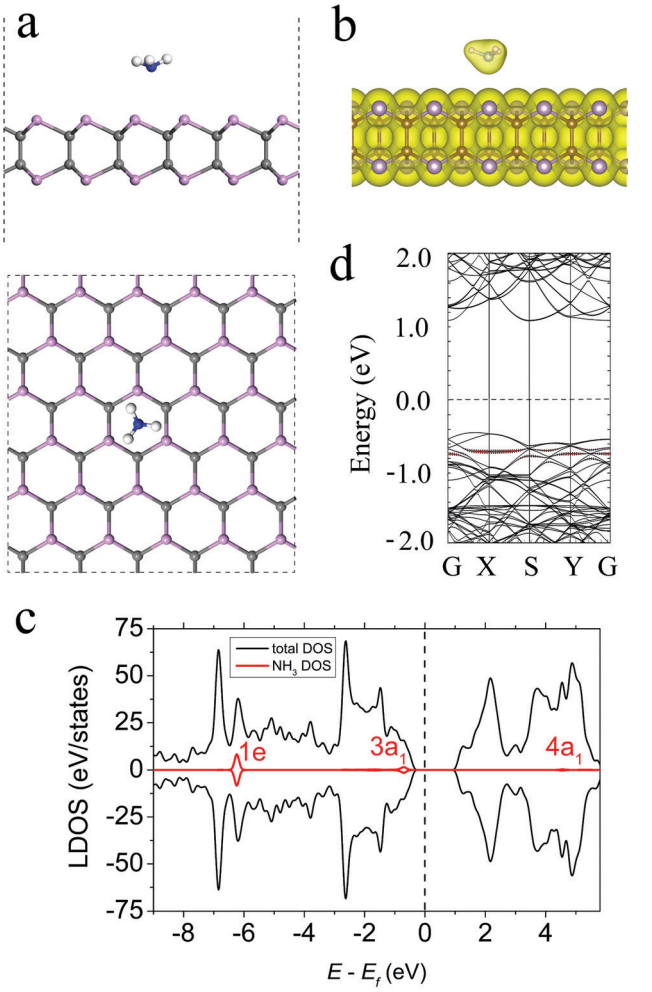

Fig. 2 (a) The side and top views, (b) total electron density plot, (c) LDOS, and (d) band structure of NH_3-adsorbed γ-PC. The black dashed line shows the Fermi level. The isosurface value is set to 0.05 e Å^{-3}. The bands and DOS coloured in red correspond to the NH_3 molecule.

The Bader charge transfer analysis indicated that NH_3 acted as an electron donor to γ-PC and the amount of charge transferred from the molecule to the surface was 0.028 *e*; however, on InSe[9] and MoS_2,[34,36] the NH_3 molecule played the role of an electron acceptor. Additional differential charge density (DCD) analysis (Fig. S4, ESI†) indicated a slight depletion of the electrons in the NH_3 molecule and the accumulation of electrons at the P atoms near the surface. This is mainly due to the ionization of the lone pair of electrons on the N atom in the $3a_1$ state. The total electron density plot (Fig. 2b) indicates the zero-electron density in the interface region between the NH_3 molecule and the γ-PC surface, which suggests non-covalent bonding between the molecule and the surface. In other considered configurations (Fig. S1, ESI†) also, NH_3 is a weak donor to γ-PC (Table S1, ESI†).

The results for the total and local density of states (LDOS) of the NH_3 molecule adsorbed on γ-PC are presented in Fig. 2c. The contribution of the molecule to the total DOS of γ-PC was far from the Fermi level, which confirmed the physisorption of NH_3 on γ-PC. The non-bonding $3a_1$ state broadened and appeared slightly below the valence band maximum (VBM); this is also seen in the band structure in Fig. 2d and reflects the charge transfer. In addition, the adsorption of the NH_3 molecule decreased the work function of γ-PC from 5.61 to 5.46 eV.

NO adsorption

For NO adsorption on γ-PC, the most energetically favourable structure is shown in Fig. 3a, where the N–O bond of the molecule is tilted to the surface and is located at d = 3.01 Å above the centre of the hexagon. The N–O bond of the molecule elongated compared to that of the free NO gas molecule from 1.010 to 1.167 Å after adsorption. This elongation of the bond is mostly attributed to the transfer of electron density from the old bond to the newly formed bond between NO and γ-PC.[35] The E_a value is −0.20 eV for NO adsorbed on γ-PC, indicating a non-covalent interaction between the molecule and the surface, which is also confirmed by the zero-electron density in the interface region between the NO molecule and the γ-PC surface (Fig. 3b). It should be noted that the E_a of NO on γ-PC was lower than that of NO on InSe[9] but was higher than that of NO on MoS_2.[34]

The Bader analysis predicted NO to be a weak electron donor to γ-PC with the amount of charge transferred from the molecule to the surface being 0.003 *e*. Interestingly, on both InSe and MoS_2, the NO molecule is an electron acceptor.[9,34] To understand this specific sensitivity of γ-PC to NO the electron localization function of the NO-adsorbed γ-PC was plotted (Fig. S5a, ESI†). It was found that there was strong charge redistribution within the molecule, while a very little amount of charge was transferred to the nearest P atom at the surface. It was also found that the acceptor/donor role of the NO molecule to γ-PC mostly depended on its position on the surface. More details are presented in ESI.†

Fig. 3c presents the LDOS of the NO molecule adsorbed on the γ-PC surface. It can be seen that the half-filled 2π frontier state is doubly degenerated and the 2π down state is located between the Fermi level and the conduction band minimum (CBM); this is also depicted in the band structure plot in Fig. 3d. The presence of unoccupied states within the band

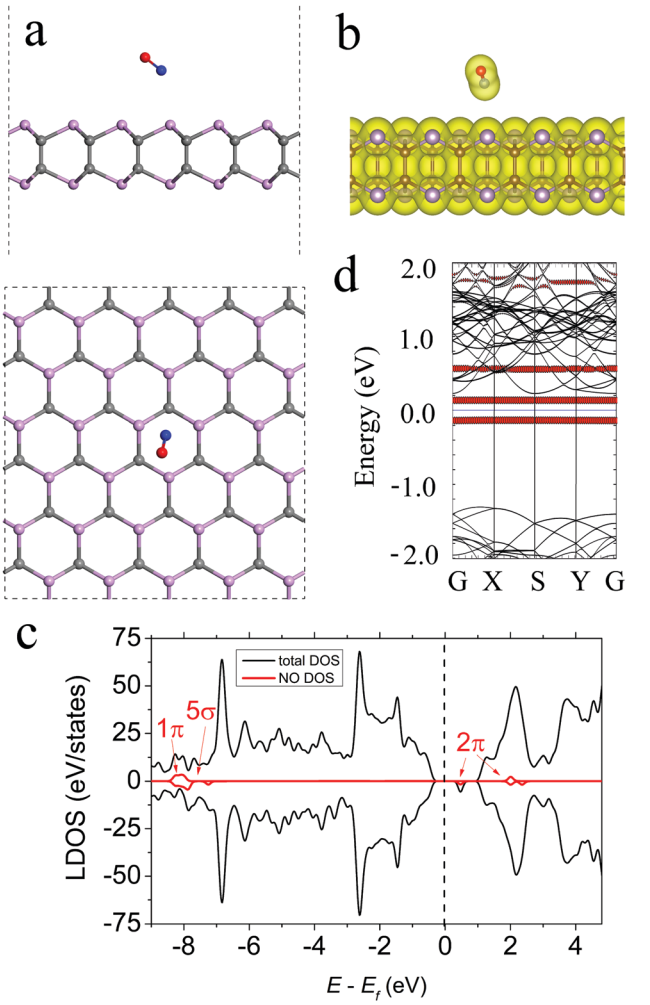

Fig. 3 (a) The side and top views, (b) total electron density plot, (c) LDOS, and (d) band structure of NO-adsorbed γ-PC. The black dashed line shows the Fermi level. The isosurface value is set to 0.05 e Å^{-3}. The bands and DOS coloured in red correspond to the NO molecule.

gap of NO-adsorbed γ-PC but a weak charge flow between the molecule and the surface may explain the significant decrease in the work function of γ-PC from 5.61 to 4.71 eV upon NO adsorption.

NO_2 adsorption

The most energetically preferable configuration of the NO_2 molecule on the γ-PC surface is shown in Fig. 4a. The molecule was located above the C–P bond at d = 2.88 Å with the N–O bonds pointing towards the surface. These N–O bonds slightly elongated to 1.217 Å compared to those of the free NO_2 gas molecule (1.20 Å). This elongation of bonds is mostly attributed to the transfer of electron density from the old bonds to the newly formed bonds between NO_2 and γ-PC.[35] The E_a value was −0.55 eV for NO_2 on γ-PC; it was ∼2.3 times lower than that of NO_2 on InSe (E_a = −0.24 eV)[9] but was ∼1.7 times higher than that of NO_2 on MoS_2 (E_a = −0.94 eV).[34] Despite the low E_a value of the NO_2 molecule on the γ-PC surface, the zero-electron density in their interface region (Fig. 4b) designates the non-covalent nature of the interaction.

The electron localization function analysis (Fig. S5b, ESI†) and the calculated charge of 0.091 *e* transferred from the γ-PC surface to the NO_2 molecule indicated the strong acceptor ability of the molecule. The charge transfer from γ-PC to NO_2 occurred through orbital hybridization, which simultaneously induced a magnetic moment of about 0.99 μ_B in γ-PC. A more detailed explanation of the acceptor nature of the NO_2 molecule on γ-PC is presented in the ESI† (Fig. S3 and Table S1). Similarly, NO_2 has been found to be a strong acceptor for InSe[9] and MoS_2.[34] The value of the work function of γ-PC remained almost unchanged after the adsorption of NO_2, which indicated that the transfer of electrons to the vacuum level was not hindered.

The LDOS and band structure, shown in Fig. 4c and d, respectively, indicate the spin splitting of the $6a_1$ orbital of NO_2 due to its adsorption on γ-PC. Particularly, the $6a_1$ spin-up state is ∼0.60 eV below the Fermi level, while the $6a_1$ spin-down state is ∼0.50 eV above the Fermi level. The $4b_1$ and $1a_2$ orbitals also exhibit spin splitting and coincide with the valence states of γ-PC. Such strong orbital mixing accounts for the charge transfer between NO_2 and γ-PC.

For applications in gas sensors and detectors, the recovery time of sensing materials is an important parameter.[28,32] Therefore, the recovery time of γ-PC was also calculated. It was found that at the room temperature of 300 K, the recovery times for NH_3, NO, and NO_2 on γ-PC were about 0.4×10^{-9}, 2.3×10^{-9}, and 2.8×10^{-3} s, respectively. This fast recovery time of γ-PC suggests that it is a promising reversible material for room-temperature gas sensors.

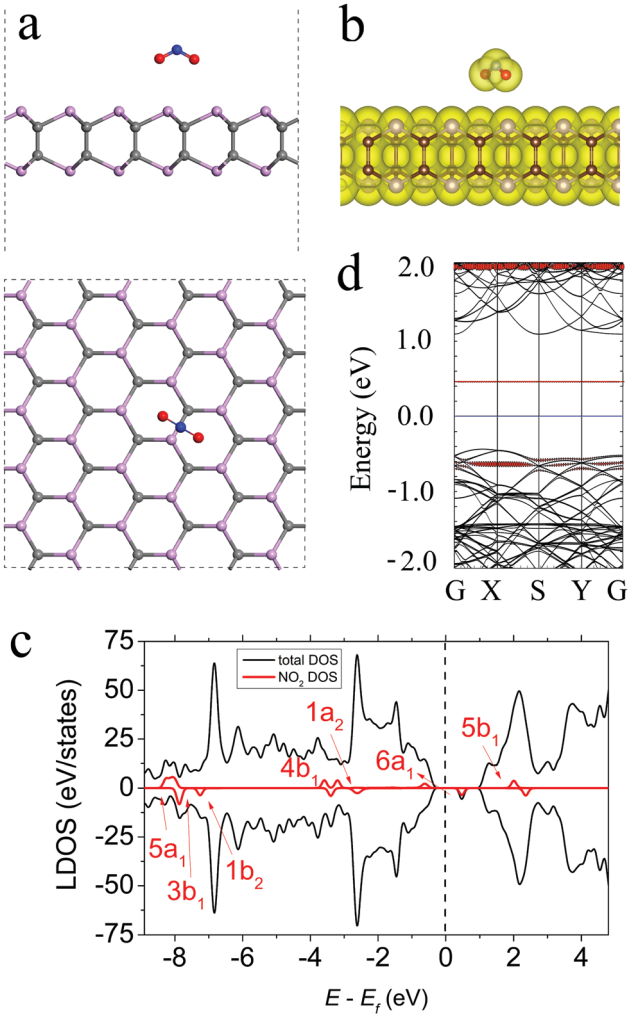

Fig. 4 (a) The side and top views, (b) total electron density plot, (c) LDOS, and (d) band structure of NO_2-adsorbed γ-PC. The black dashed line shows the Fermi level. The isosurface value is set to 0.05 e Å^{-3}. The bands and DOS coloured in red correspond to the NO_2 molecule.

Methods

The simulations were based on the density functional theory (DFT), as implemented in the Vienna *ab initio* simulation package (VASP).[37] The exchange correlation interaction was described by the generalized gradient approximation (GGA) with the Perdew, Burke and Ernzerhof (PBE) functional.[38] The hybrid Heyd–Scuseria–Ernzerhof (HSE06) functional was employed for the test calculations of the electronic structure of the γ-PC unit cell.[39] To obtain a better description of the long-range van der Waals interactions between the surface and gas molecules, the van der Waals-corrected functional with Becke88 optimization was used. The Brillouin zone sampling for *k*-points was based on a 6 × 6 × 1 Monkhorst–Pack grid. The atomic positions were relaxed until the force on each atom was smaller than 0.01 eV Å^{-1}. The simulated system of a 5 × 3 × 1 supercell was created with the vacuum space in the *z*-direction larger than 15 Å to avoid interactions with the neighbouring super cells. The kinetic energy cut-off for the plane wave expansion was set to 400 eV. The adsorption energy of gas molecules on the γ-PC surface was calculated as follows:

$$E_a = E_{PC/mol} - E_{PC} - E_{mol}, \quad (1)$$

here, $E_{PC/mol}$ is the total energy of the molecule-adsorbed γ-PC system, and E_{PC} and E_{mol} are the total energies of pristine γ-PC and a free gas molecule, respectively.

Bader analysis[40] was conducted to estimate the charge flow between the γ-PC surface and gas molecules. The work function was calculated as the difference between the electrostatic potentials of an electron at points remote from the surface and the Fermi level.

According to the conventional transition state theory, the recovery time[32,41] (τ) can be expressed as follows:

$$\tau = \nu^{-1} e^{(-E_a/K_B T)}, \quad (2)$$

here, T is the temperature, K_B is the Boltzmann constant, ν is the attempt frequency (10^{12} s^{-1}),[41] and the desorption energy barrier can be approximated as the adsorption energy E_a.[32,41]

Conclusions

The calculated low adsorption energies of the NH_3, NO, and NO_2 molecules on the γ-PC surface suggested strong interactions between γ-PC and these molecules. In all the considered cases, the molecules were physiosorbed on γ-PC, which suggested that

they may easily desorb from its surface. Due to this, γ-PC possessed a short recovery time. In addition, the adsorption abilities of NH_3, NO, and NO_2 on γ-PC were superior to those on InSe but lower than those on MoS_2. The physisorption of NO and NO_2 led to a remarkable change in the band structure of γ-PC. Hence, the presence of these molecules on its surface could be detected. Moreover, the physisorption of NH_3 and NO induced significant modulations in the work function of γ-PC.

Conflicts of interest

There are no conflicts to declare.

Acknowledgements

The author acknowledges CSC – IT Center for Science, Finland, for computational resources and the financial support provided by the Academy of Finland (grant No. 311934).

Notes and references

1 S. A. Wells, A. Henning, J. T. Gish, V. K. Sangwan, L. J. Lauhon and M. C. Hersam, *Nano Lett.*, 2018, **18**, 7876.
2 Q. Li, Q. Zhou, L. Shi, Q. Chen and J. Wang, *J. Mater. Chem. A*, 2019, **7**, 4291.
3 D. C. Elias, R. R. Nair, T. M. G. Mohiuddin, S. V. Morozov, P. Blake, M. P. Halsall, A. C. Ferrari, D. W. Boukhvalov, M. I. Katsnelson, A. K. Geim and K. S. Novoselov, *Science*, 2009, **323**, 610.
4 L. Kou, T. Frauenheim and C. Chen, *J. Phys. Chem. Lett.*, 2014, **5**, 2675.
5 S. Zhao, J. Xue and W. Kang, *Chem. Phys. Lett.*, 2014, **595**, 35.
6 T. Järvinen, G. S. Lorite, J. Peräntie, G. Toth, S. Saarakkala, V. K. Virtanen and K. Kordas, *Nanotechnology*, 2019, **30**, 40550.
7 D. Ma, W. Ju, Y. Tang and Y. Chen, *Appl. Surf. Sci.*, 2017, **426**, 244.
8 S. Yang, C. Jiang and S. Wei, *Appl. Phys. Rev.*, 2017, **4**, 021304.
9 Y. Cai, G. Zhang and Y. W. Zhang, *J. Phys. Chem. C*, 2017, **121**, 10182.
10 A. A. Kistanov, Y. Cai, K. Zhou, S. V. Dmitriev and Y. W. Zhang, *J. Mater. Chem. C*, 2018, **6**, 518.
11 Y. Cai, Q. Ke, G. Zhang and Y. W. Zhang, *J. Phys. Chem. C*, 2015, **119**, 3102.
12 J. Park, J. Mun, J. S. Shin and S. W. Kang, *R. Soc. Open Sci.*, 2018, **5**, 181462.
13 M. Schleicher and M. Fyta, *ACS Appl. Electron. Mater.*, 2020, **2**, 74.
14 F. Safaria, M. Moradinasab, M. Fathipour and H. Kosina, *Appl. Surf. Sci.*, 2019, **464**, 153.
15 A. N. Abbas, B. Liu, L. Chen, Y. Ma, S. Cong, N. Aroonyadet, M. Köpf, T. Nilges and C. Zhou, *ACS Nano*, 2015, **9**, 5618.
16 Gaganpreet, *Appl. Surf. Sci.*, 2020, **507**, 144967.
17 S. Kuriakose, T. Ahmed, S. Balendhran, V. Bansal, S. Sriram, M. Bhaskaran and S. Walia, *2D Mater.*, 2018, **5**, 032001.
18 D. R. Kripalani, Y. Cai, M. Xue and K. Zhou, *Phys. Rev. B*, 2019, **100**, 224107.
19 B. Liu and K. Zhou, *Prog. Mater. Sci.*, 2019, **100**, 99.
20 A. A. Kistanov, S. K. Khadiullin, K. Zhou, S. V. Dmitriev and E. A. Korznikova, *J. Mater. Chem. C*, 2019, **7**, 9195.
21 J. Jin, Y. Zheng, S. Huang, P. Sun, N. Srikanth, L. B. Kong, Q. Yan and K. Zhou, *J. Mater. Chem. A*, 2019, **7**, 783.
22 J. Guan, D. Liu, Z. Zhu and D. Tománek, *Nano Lett.*, 2016, **16**, 3247.
23 A. Furlana, G. K. Gueorguiev, Z. Czigány, V. Darakchieva, S. Braun, M. R. Correia, H. Högberg and L. Hultman, *Thin Solid Films*, 2013, **548**, 247.
24 G. Wang, R. Pandey and S. P. Karna, *Nanoscale*, 2016, **8**, 8819.
25 W. C. Tan, Y. Cai, R. J. Ng, L. Huang, X. Feng, G. Zhang, Y. W. Zhang, C. A. Nijhuis, X. Liu and K. W. Ang, *Adv. Mater.*, 2017, **29**, 1700503.
26 K. P. Katin, V. S. Prudkovskiy and M. M. Maslov, *Phys. Lett. A*, 2017, **381**, 2686.
27 K. P. Katin, V. S. Prudkovskiy and M. M. Maslov, *Physica E*, 2016, **81**, 1.
28 D. Ma, W. Ju, T. Li, G. Yang, C. He, B. Ma, Y. Tang, Z. Lu and Z. Yang, *Appl. Surf. Sci.*, 2016, **371**, 180.
29 B. Cho, *et al.*, *Sci. Rep.*, 2015, **5**, 8052.
30 S. Posysaev and M. Alatalo, *ACS Omega*, 2019, **4**, 4023.
31 J. Z. Ou, W. Ge, B. Carey, T. Daeneke, A. Rotbart, W. Shan, Y. Wang, Z. Fu, A. F. Chrimes, W. Wlodarski, S. P. Russo, Y. X. Li and K. Kalantarzadeh, *ACS Nano*, 2015, **9**, 10313.
32 D. Ma, J. Zhang, X. Lia, C. Heb, Z. Lu, Z. Luc, Z. Yang and Y. Wang, *Sens. Actuators, B*, 2018, **266**, 664.
33 W. Zhang, J. Yin, P. Zhang, X. Tang and Y. Ding, *J. Mater. Chem. A*, 2018, **6**, 12029.
34 L. Kou, A. Du, C. Chen and T. Frauenheim, *Nanoscale*, 2014, **21**, 5156.
35 A. Abbasi and J. J. Sardroodi, *Appl. Surf. Sci.*, 2019, **469**, 781.
36 Q. Yue, Z. Shao, S. Chang and J. Li, *Nanoscale Res. Lett.*, 2013, **8**, 425.
37 G. Kresse and J. Furthmüller, *Phys. Rev. B: Condens. Matter Mater. Phys.*, 1996, **54**, 11169.
38 A. D. Becke, *Phys. Rev. A: At., Mol., Opt. Phys.*, 1988, **38**, 3098.
39 J. Heyd, G. E. Scuseria and M. Ernzerhof, *J. Chem. Phys.*, 2003, **118**, 8207.
40 R. F. W. Bader, *Atoms in Molecules – A Quantum Theory*, Oxford University Press, New York, 1990.
41 B. Roondhea and P. K. Jha, *J. Mater. Chem. B*, 2018, **6**, 6796.